

CAPABILITY OF ASTEC V2.1 TO SIMULATE A SEVERE ACCIDENT IN A NUCLEAR POWER PLANT – APPLICATION TO A TMI-2-LIKE ACCIDENT SCENARIO

P.Drai¹, P.Chatelard¹, L.Laborde¹, L. Piar¹, F. Fichot¹, G.Brillant¹

¹ Institut de Radioprotection et de Sûreté Nucléaire (IRSN)

Nuclear Safety Division/Safety Research/Severe Accident Department

Saint Paul Lez Durance, 13115, France

Patrick.drai@irsn.fr ; patrick.chatelard@irsn.fr; laurent.laborde@irsn.fr ; libuse.piar@irsn.fr ;
florian.fichot@irsn.fr ; guillaume.brillant@irsn.fr

ABSTRACT

ASTEC is an integral code for the prediction of Severe Accidents in Nuclear Power Plants. As such, it has to cover all physical processes that could occur during accident progression, and to produce results within an acceptable time.

The present paper is about the newest capabilities of ASTEC V2.1 version with a focus on an original reflooding model devoted to both a rod-like geometry representative of a quasi-intact core and severely degraded situations in the core including debris bed and molten pool with local flow blockages.

Indeed, reflooding is an important accident measure to stop the progression of a severe accident and it leads to molten material solidification, debris components formation and additional hydrogen production. In order to predict accurately phenomena occurring during the reflooding phase, an original model developed initially in the ICARE/CATHARE V2 IRSN code has been improved and implemented in ASTEC V2.1.

The first part of this paper will present the reflooding model, the second one is devoted to its validation on the PERICLES experimental facility and the last one will concern an ASTEC V2.1 calculation on a power plant calculation. The scenario retained and the geometry chosen for this power plant application is the TMI-2 real scenario.

KEYWORDS

ASTEC, core degradation, core thermal-hydraulics, reflooding, late phase modeling, TMI-2

1. INTRODUCTION

One of the main goals of the ASTEC V2.1 [1] new version concerns the capability to model nuclear power plant accident with water injections and core reflooding during the scenario. Indeed, reflooding is the main accident management measure to take in order to stop the progression of a severe accident in a light water reactor (LWR). However, it remains difficult to predict the effects of reflooding in a core at very high temperatures where the core might have been significantly damaged. Some difficulties come from the incomplete knowledge of the possible enhancement of Zircaloy oxidation caused by the strong steam production during reflooding. But other difficulties come from the uncertainties in the basic

understanding and modelling of the flow and heat transfers across the fuel assemblies, whether damaged or not.

Most of the codes used for severe accident calculations, in particular for Probabilistic Safety Analysis (PSA) studies, must use rather large meshes (tens of cm) in order to keep the computation time reasonable. Therefore, they cannot benefit from models developed recently, taking into account phenomena occurring at a very small scale like the axial heat conduction in the solid structure. The present paper introduces a model developed previously in ICARE/CATHARE V2 IRSN code [2] that takes advantage of experimental observations of the structure of the two-phase flow in the near quench front [3].

The basic idea of the model is to calculate an integrated heat flux over the mesh where the quench front is located, instead of calculating a heat transfer coefficient which is not the relevant parameter in such situation. In order to be consistent, the model requires an accurate tracking of the quench front position, which is done thanks to a method similar to the enthalpy method used to solve Stefan's problem (front tracking method on a fixed grid). The new model is assessed by comparing the predicted results with experimental data obtained in the large scale tests PERICLES (CEA, France, [4]) and RBHT (PSU, USA, [5]). An application to this model on the real TMI-2 scenario is presented in the last part of this paper.

2. REFLOODING MODEL DESCRIPTION

Reflooding is the main accident management measure in order to stop the progression of a severe accident in a light water reactor (LWR). During the severe accident at the Three Mile Island Unit 2 (TMI-2), 50% of the reactor core was molten, of which 30% had relocated down into the lower plenum [11]. It is characterized by the injection of large amounts of water on the very hot structures of the core. The resulting flow pattern is usually split into four zones (see Figure 1):

- below the quench front, all the temperatures are under the burn-out temperature and the walls are wet;
- just above the quench front, a non-stable two-phase flow establishes at the wall side; there, very large axial temperature gradients can influence the cooling (top-bottom conductive heat transfers);
- further above, a stable gaseous film establishes along the walls, limiting drastically the coolability of the structures (inverted annular flow);
- far above the quench front, the gas phase is predominant with droplets and/or water slugs.

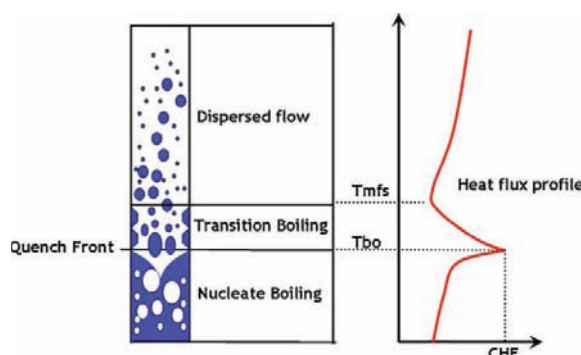


Figure 1: Flow regimes during reflooding

This reflooding model is only devoted to bottom-top reflooding (i.e. with ascending water). And it is assumed that the core geometry is sufficiently intact to be properly treated by a mono-dimensional approach. But in case of a transition to a severe degraded configuration like debris bed or molten pool inside the core, this model has been adapted thanks to head-losses coefficients taking into account the new geometry. In the future, a specific model devoted to porous media, and currently under development, will be used for late phase configurations.

The model is automatically activated when a quench front is found. The exact position of the quench front is then estimated explicitly and some modifications are performed in convective heat exchanges.

The reflooding model is fully driven by the quench front location, which is estimated explicitly.

A schematic evolution of wall temperature evolution (around the quench front) as a function of vertical elevation is represented in Figure 2 and Figure 3.

Experimental results indicate that, in the quench front region, the clad temperature increases by 200 K on a short length (about 5 cm, [3] [6]). For reactor transient calculations, the typical mesh size is about 25 cm. That is why the description of the transition boiling region is difficult. Indeed, heat flux in a large mesh containing the quench front is generally strongly under-estimated.

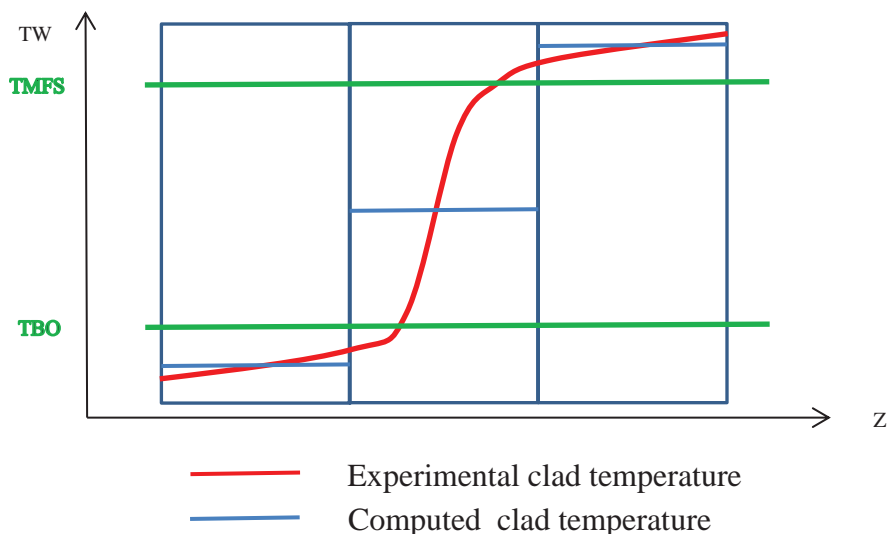


Figure 2: Temperature profile around the quench front

In each hydraulic channel, it is considered that the quench front is located in the first mesh (starting from the bottom of the rods) where the clad temperature is greater than the burn-out temperature (critical heat flux temperature) and the void fraction is greater than $\alpha_{\max} = 0,99$ (parametric value).

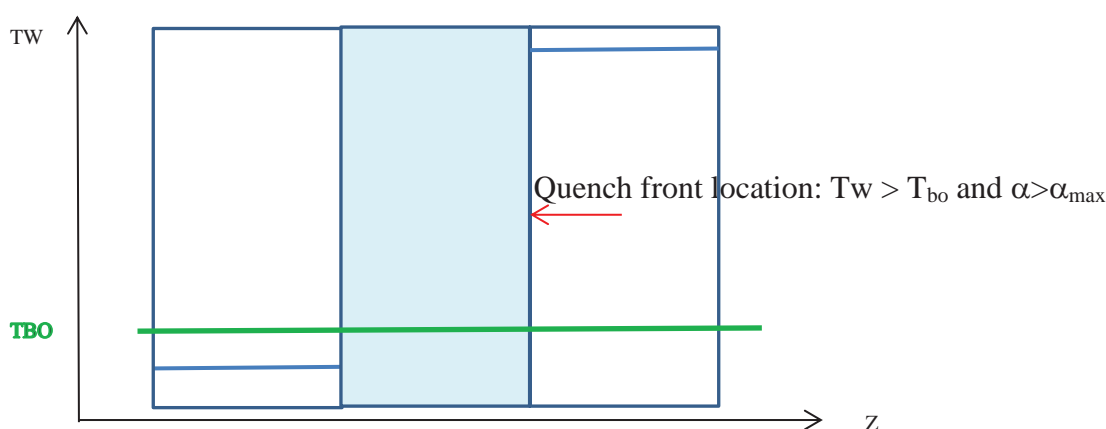


Figure 3: Quench front location

The burn-out temperature T_{bo} is defined as follows:

$$T_{bo} = T_{sat} + \left(\frac{CHF}{H_{en}} \right)^{0,5}$$

With :

T_{sat} : saturation temperature
 CHF : critical heat flux
 H_{en} : heat transfer for nucleate boiling
 P : Pressure

$$H_{en} = 1,97 \cdot 10^3 \cdot e^{0,23P \cdot 10^{-6}}$$

To compute the quench front location, it is assumed that the wall temperature profile is evolving like a step (Figure 4): T^- and T^+ are respectively the wall temperature in the meshes downstream and upstream from the one where the quench front position is located, named Z_{QF} . T_{ZQF} is the temperature in the mesh where the quench front is located and is used in a relationship for determining quench front location :

$$T_{ZQF} = L Z_{QF} T^- + (1 - Z_{QF} \cdot L) T^+ \quad \begin{matrix} L \text{ length of the mesh} \\ 0 < Z_{QF} < 1 \text{ (0 at the bottom, 1 at the top of the mesh)} \end{matrix}$$

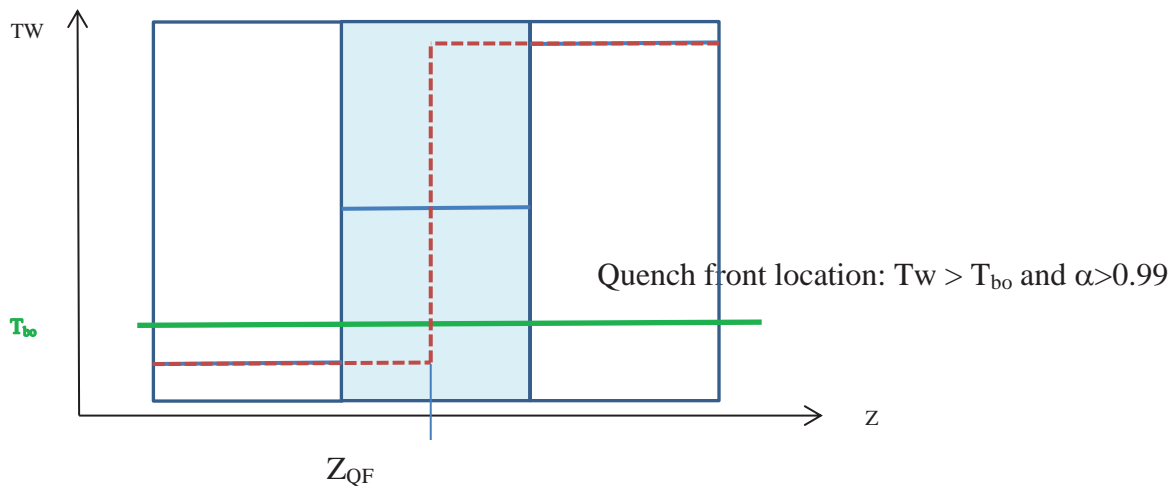


Figure 4: Clad temperature modelling

The wall to fluid heat transfer around the quench front Φ_{TB} is described in Figure 5.

Wall-fluid heat flux profile

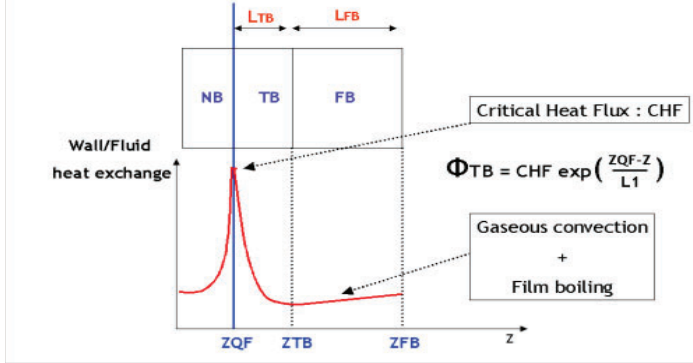


Figure 5: Heat flux profile in the transition boiling zone

At the quench front, the heat flux is equal to the critical heat flux CHF. Downstream, the flux decreases exponentially with respect to the distance to the quench front. A characteristic length L_1 is obtained thanks to Ishii experiments [8] and proportional to the square root of the capillarity number Ca .

$$Re < 2000, L_1 = \frac{5}{8} Ca^{0.5}$$

$$Re > 2000, L_1 = Ca^{0.5}$$

The heat flux in the transition zone is defined as follows:

$$\Phi_{TB} = CHF \cdot e^{-\frac{Z_QF-Z}{L_1}}$$

In the film boiling regime, the heat exchange between the wall and the two phase fluid is the sum of two terms:

Φ_{CG} : gaseous convection between wall and gas

Φ_{FB} : film boiling (droplet and continuous phase) heat exchange.

3. VALIDATION OF THE REFLOODING MODEL ON THE PERICLES EXPERIMENTAL FACILITY

In order to assess ASTEC V2.1 reflooding model, a comparison with the whole matrix of PERICLES core reflooding tests has been realized. Two kinds of tests have been carried out, named respectively low pressure tests (3 bar) and high pressure tests (10 to 60 bar). The main physical parameters varying between tests are mass flow rate injection (1 to 19 g/cm/s) and power (1 to 4.2 W.cm⁻²).

3.1. General presentation of PERICLES facility

The PERICLES experimental program was performed in CEA between 1983 and 1988 [4] for simulating situations like a core uncover situation, a core reflooding situation and an intermediate situation named boiling in which the core keeps a constant value. The test section simulates a PWR fuel assembly including a guide thimble installed on a thermal insulated cylindrical shroud. Each fuel pin simulator is

heated thanks to electrical power, with an axial peaking factor equal to 1.6. The external cladding is made of stainless steel.

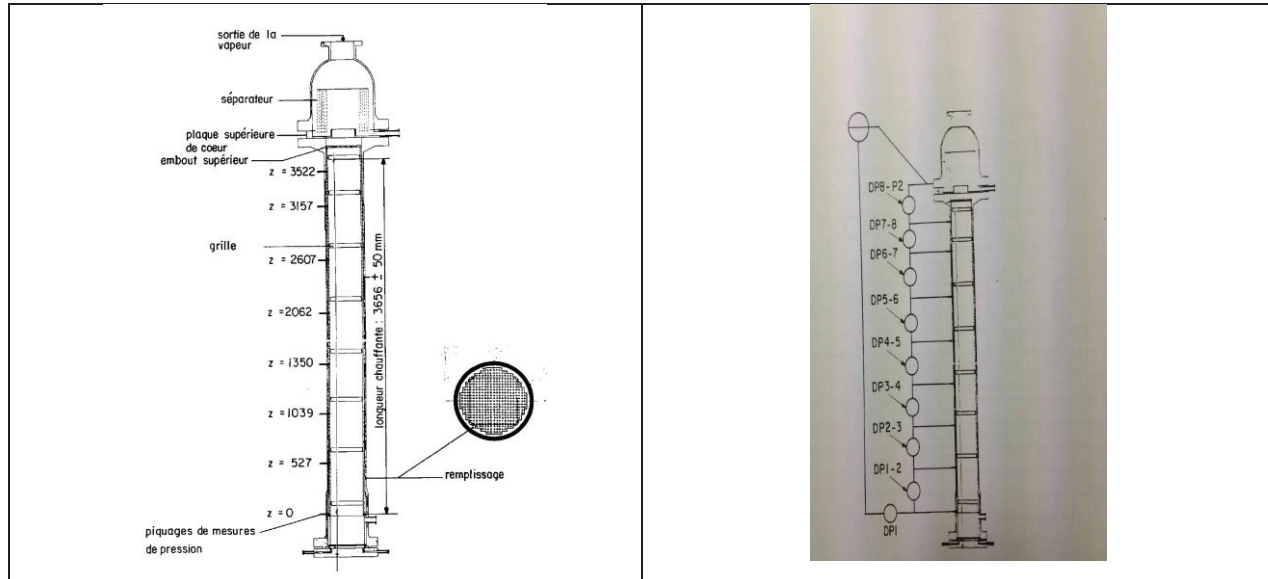


Figure 6: PERICLES Test facility

The whole bundle includes 124 instrumented heaters rods with temperature sensors located at several elevations. Water collapsed level is calculated from pressure drop evolution (Figure 6.) and swollen level is deduced from cladding profile temperature like in the experiment.

3.1. Reflooding conditions

Initially a low steam mass flow rate flows through the bundle. During the test, the system pressure is kept constant. Afterwards, the test is performed in this way: power supply is activated; as soon as the maximum cladding temperature in the central part of the bundle reaches the value required (600K), reflooding from the bottom occurs. The test ends when the bundle is reflooded.

The test matrix is presented in the Tables I and II hereafter:

Table I. Experimental conditions for PERICLES high pressure tests

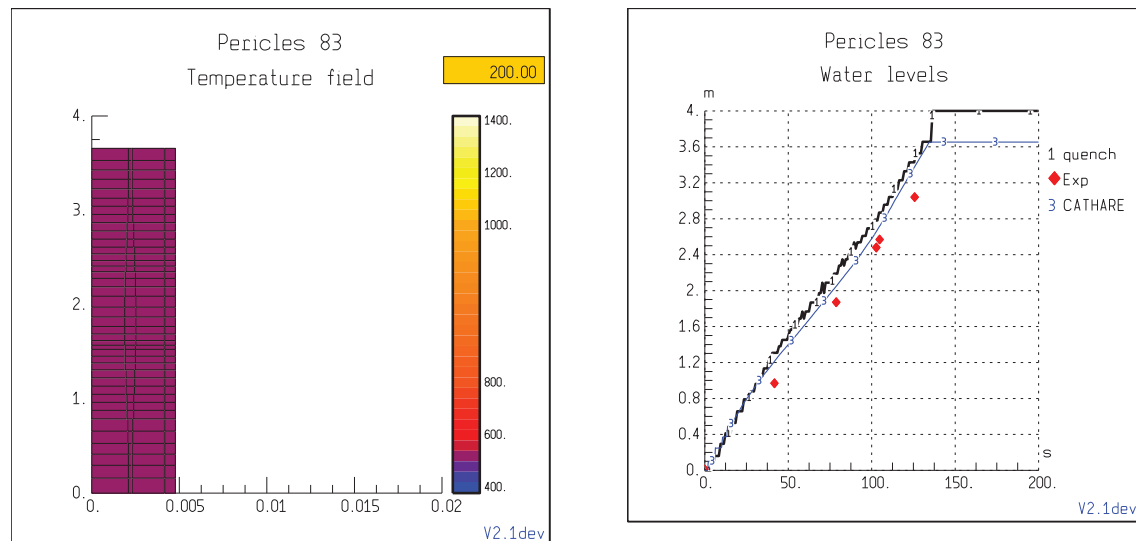
Tests	Nominal Pressure (bar)	Heat flux (W.cm ⁻²)	Water injection Mass flow rate (g.cm ⁻² .s ⁻¹) - T≈Tsat-5K
74	20.	2.	3.
75	40.	2.	3.
77	10.	1.	3.
82	40.	1.	3.
83	60.	2.	3.

Table II. Experimental conditions for PERICLES low pressure tests

Tests	Nominal Pressure (bar)	Heat flux (W.cm ⁻²)	Water injection Mass flow rate (g.cm ⁻² .s ⁻¹) - T≈Tsat-60K
1	3.	3.35	3.6
3	3.	1.5	1.
5	3.	3.35	2.5
7	3.	3.35	5.
8	3.	3.35	6.
14	3.	3.35	19.
25	3.	4.2	25.

3.3. ASTEC V2.1 calculation

A comparison between ASTEC calculation results, measured values and CATHARE code [7] (CATHARE is the FRENCH reference computer code used in thermal-hydraulics in the framework of PSA studies) calculation has been realized for the whole test matrix [9]. One radial mesh and 40 axial meshes are used in the ASTEC calculation. Two of these comparisons are presented hereafter: on the PERICLES 83 high pressure test (Figure 7.) and on the PERICLES 5 low pressure test (Figure 8.). The first evolution corresponds to ASTEC V2.1 calculation, the second one to the experimental measured values and the third one comes from a CATHARE code calculation. Results for clad temperature evolution at several elevations, water level evolution and pressure drop are in very good accordance.



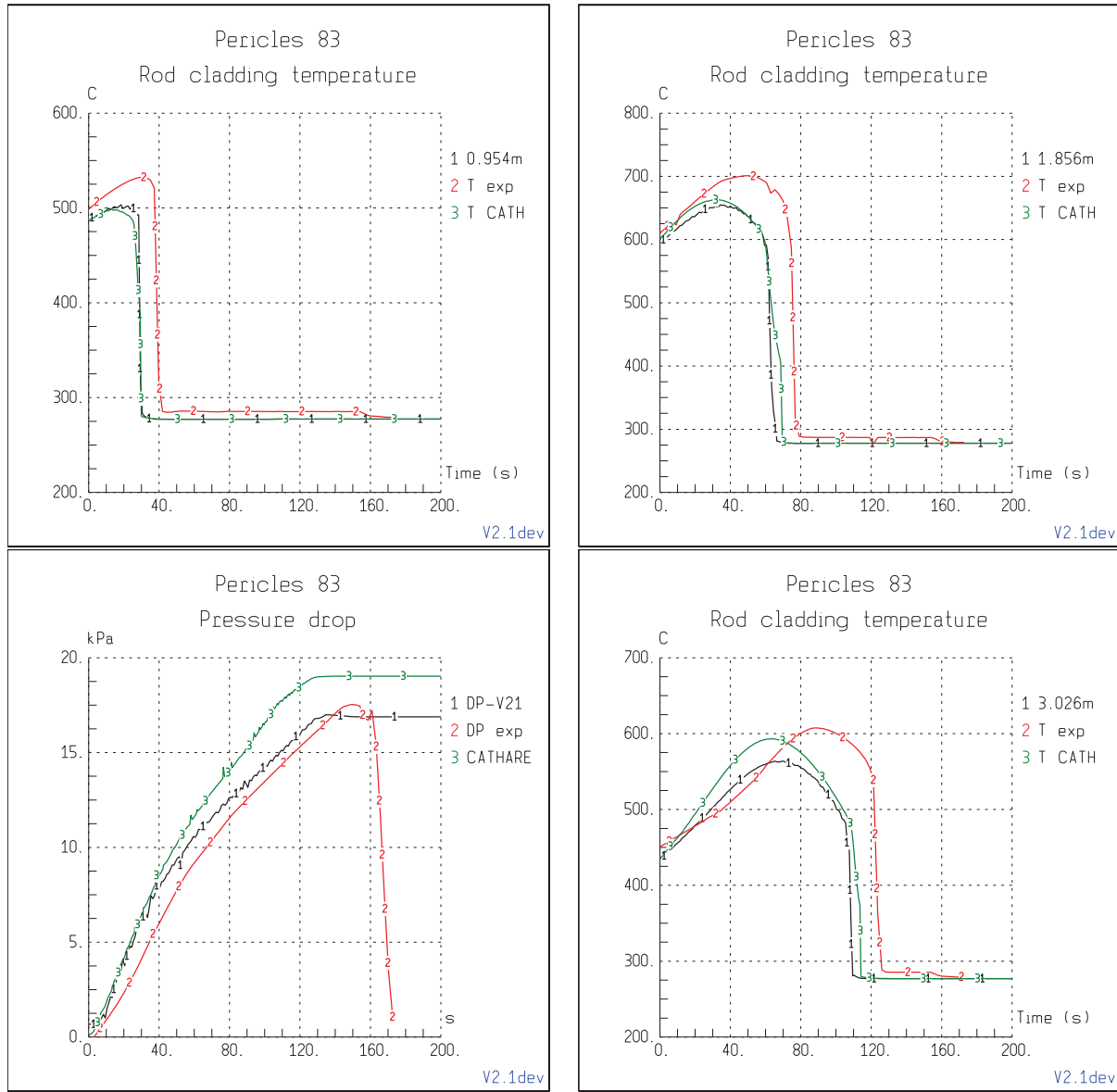


Figure 7: PERICLES 83 – high pressure test

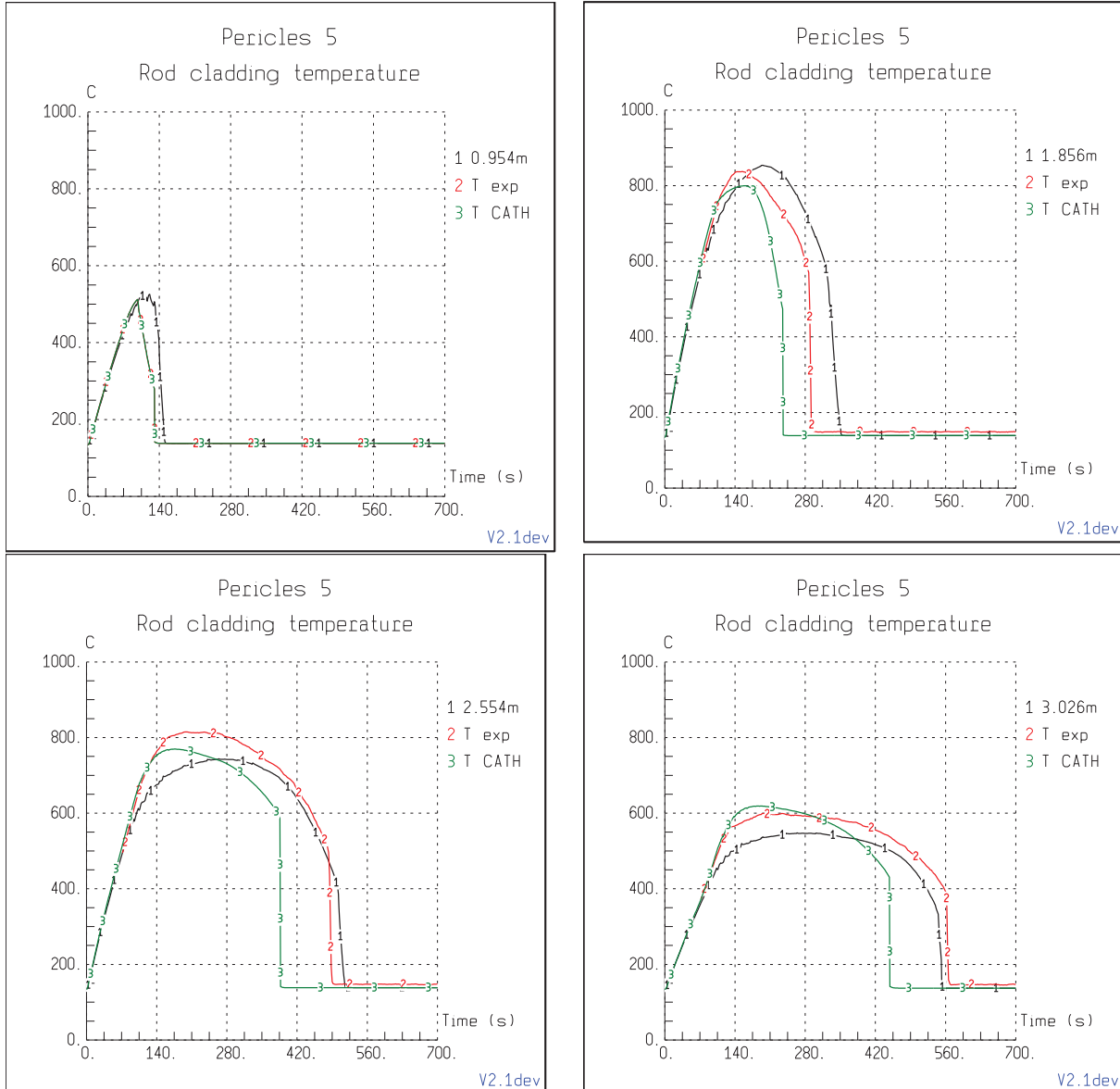


Figure 8: PERICLES 5 – low pressure test

Comparison for both tests reveals a good agreement between measured values, CATHARE code [7] and ASTEC V2.1 calculations. A detailed analysis for all the calculations is provided in [9].

Calculations have also been realized for both QUENCH 3 and QUENCH 11 tests [10], with a very good agreement between ASTEC calculation and experimental measured values. These results are important because they validate the use of this reflooding model for degraded situations into the core region.

4. VALIDATION OF THE REFLOODING MODEL ON TMI-2 REAL SCENARIO

4.1. Steady state calculation

In order to calculate accurately the accidental scenario, it is necessary to check the main parameters of the steady state in order to ensure that steady state is reached in accordance with measured values before the

accident. The Figure 9 illustrates evolutions of some parameters like primary mass flow rate, primary temperature at the hot leg, primary and secondary pressure and steam generator mass flow rate with a perfect agreement between the code and expected values. Other parameters have also been checked with an excellent agreement (Table III).

Table III. Main parameters for TMI2 steady state

	ASTEC V2.1	TMI-2
Nuclear power (MW)	2700.	2700.
Primary pressure (bar)	151.7	152.
Pressurizer level (m)	5.77	5.77
Primary mass	231.9	230.4
SGA level (m)	5.29	--
SGB level (m)	5.38	--
Steam temperature SGA (K)	584.	586.
Steam temperature SGB (K)	581.	586.

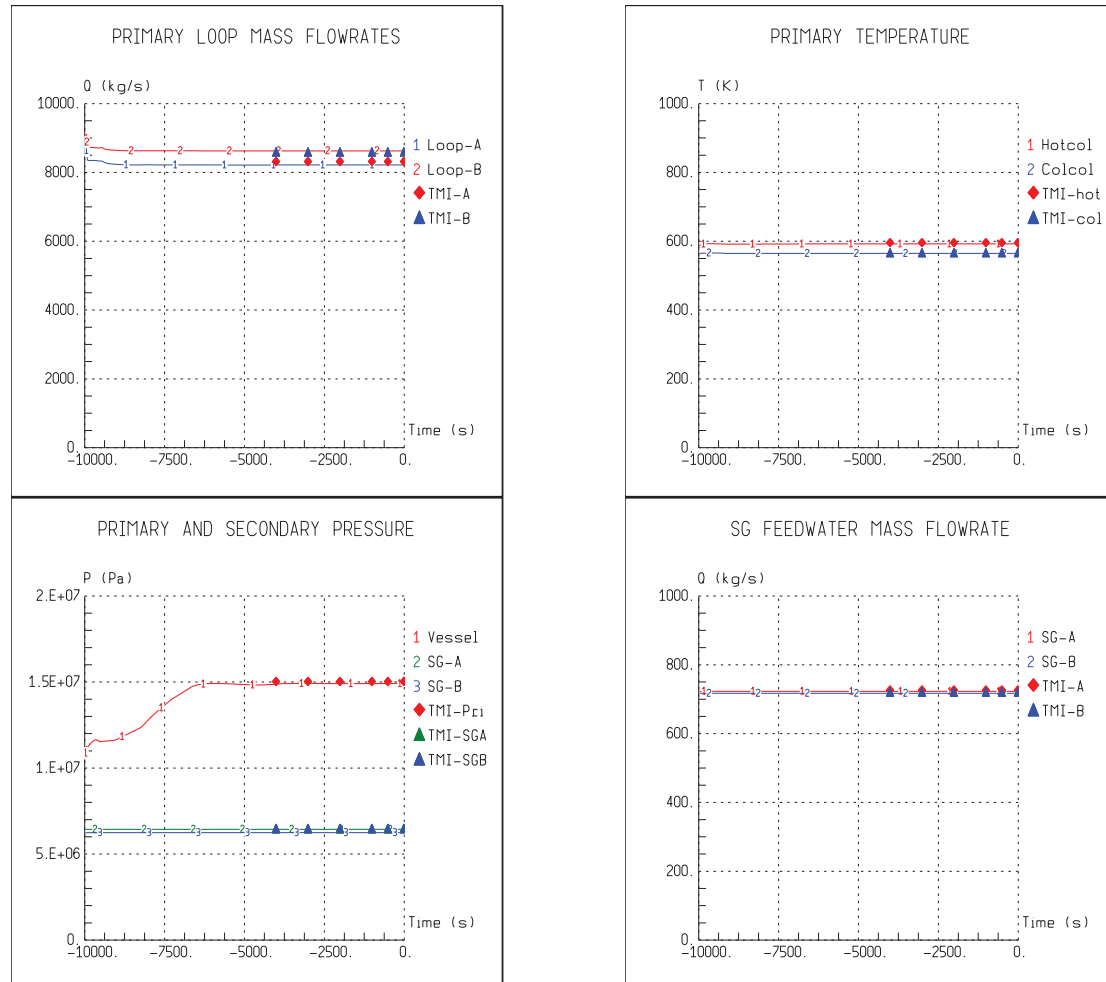


Figure 9: TMI2 – steady state calculation

4.2. Transient calculation

The accidental scenario [11] starts with a loss of feed water ($t=0$ s) leading to a peak of pressure in the primary circuit and to a pressurizer relief valve opening ($t=3$ s) represented in Figure 11, evolution 5. This peak of pressure induces a SCRAM at time 9s (Figure 10).

Table IV. Main events for TMI2 accidents

TIME (s)	ASTEC V2.1	TMI-2 [8]
Stop ARE	0	0
PORV opening	3.	3.
SCRAM	9.2	9
Start Safety Injection (SI)	122.	121
Stop SI	278.	278
SGA start	498.	498
Stop GMPP A	4409	4380
Stop GMPP B	6045	6000
PORV closure	8520	8520
First slumping into lower plenum	7919	?
Start GMPP B	10440	10440
PORV opening	11548	11548
Start SI	12000	12000
Stop of calculation	15000	-----

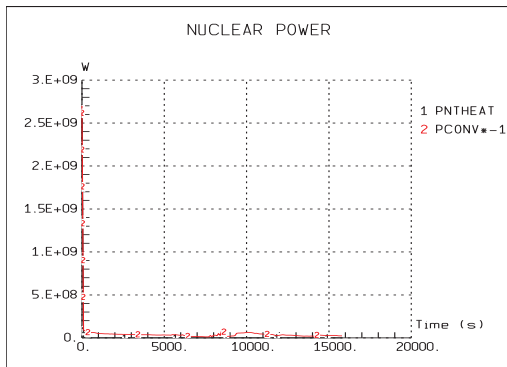


Figure 10: Nuclear and convective power

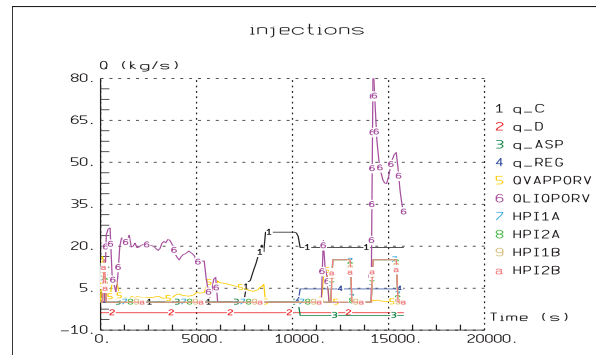


Figure 11: Injections

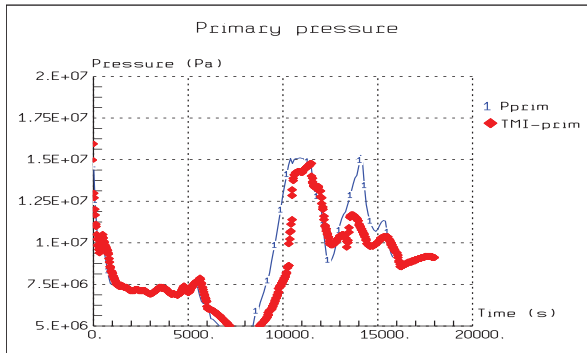


Figure 12. Primary pressure evolution

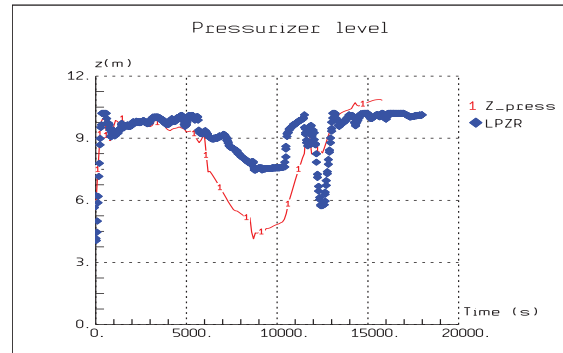


Figure 13. Pressurizer level

Because of PORV opening, primary pressure decreases (Figure 12, evolution 1) and when pressure reaches 110 bar, safety injection is activated at time 121s (Figure 11, evolutions 7,8,9,10).

Then, at time 278s and because of a high level of water in pressurizer (Figure 13, evolution 1), safety injection is manually closed. Then, at time 498s, auxiliary feed water is activated manually on the secondary side.

Primary pumps are stopped respectively at times 4380s (GMPPA) and 6000s (GMPPB) because of cavitation in the primary loop leading to alarms in the control room. These events lead to a strong decrease of the primary mass flow rate (Figure 14, evolutions 1,2).

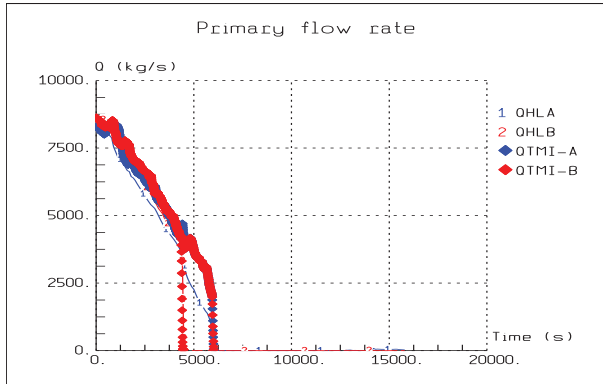


Figure 14: Primary mass flow rate

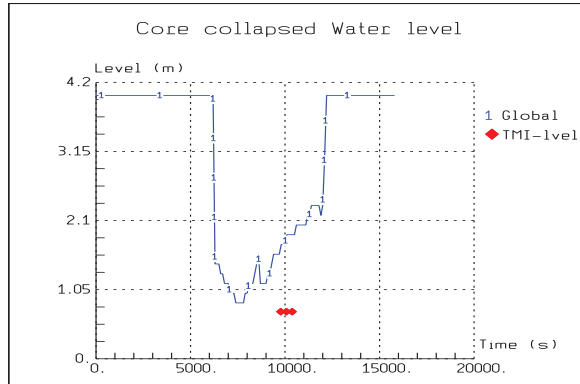


Figure 15 : Core level

One has to notice that the pressurizer level is too low just after the stop of GMPP B. Indeed, pressurizer water flows to the hot leg, whereas this phenomenon was not observed in the reality.

The same kind of behavior has ever been observed in previous studies realized with both ICARE/CATHARE code and CATHARE code only with no real explanations; It was supposed that interfacial friction terms were not well adapted for TMI-2 configuration and fictive valve was defined in order to cancel pressurizer discharge. This solution has not been retained in this calculation.

Furthermore, the stop of the primary pumps lead to a strong vaporization in the core at time 6000s when GMPPB is stopped and to a core uncover. (Figure 15: evolution 1).

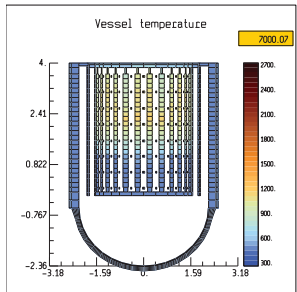


Figure 16 a) $t=7000$ s

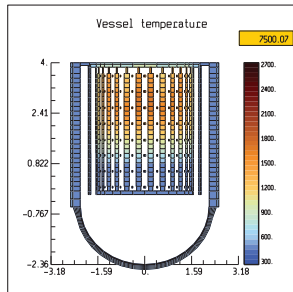


Figure 16 b) $t=7500$ s

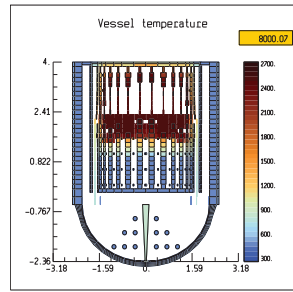


Figure 16 c) $t=8000$ s

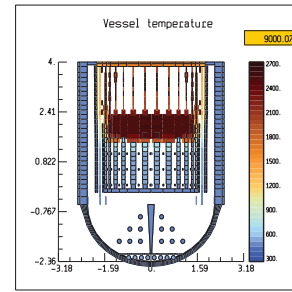


Figure 16 d) $t=9000$ s

Because of the core uncoverage, convective heat transfers between fuel rods and steam induce a strong temperature increase up to the melting of core components and relocation of molten materials (Figure 16 a,b,c,d).

Degradation of the core is stopped by water level not below than 0.9 meter of elevation.

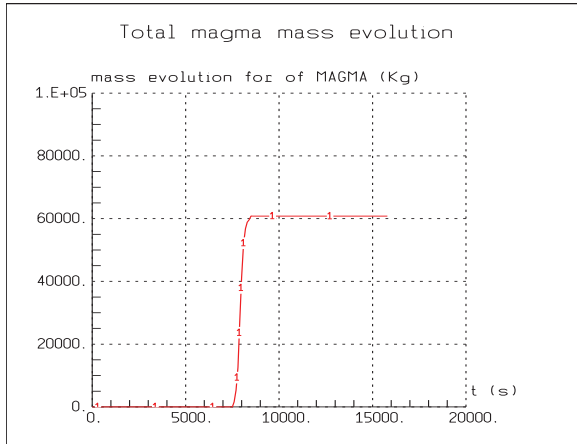


Figure 17: total amount of molten components

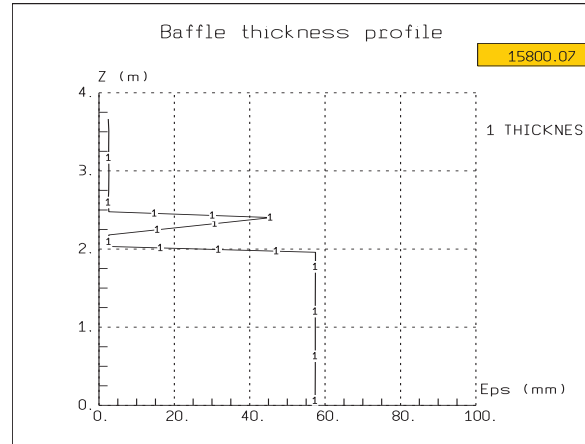


Figure 18: baffle thickness profile

The main evolution of the degradation occurs between time $t=7000$ s and time $t=9000$ s (Figure 17). The first slumping into the lower head happens at time $t=7919$ s through the bypass at elevation $z=2$ m (Figure 18, same observation for elevation in TMI-2 real scenario).

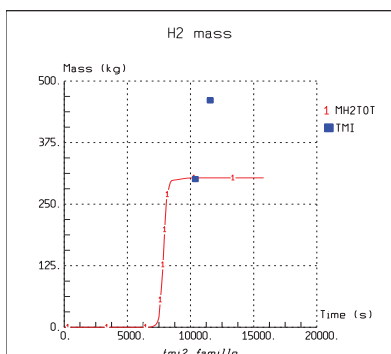


Figure 19: total amount of hydrogen production

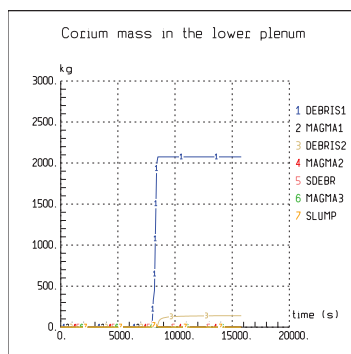


Figure 20: magma mass in the lower plenum

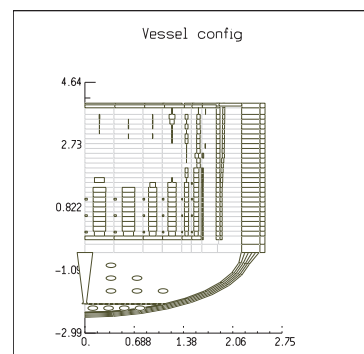


Figure 21: vessel config at end of calculation

The total mass of molten materials reaches 60 tons and corresponds to the total amount of magma and relocated components measured in the TMI-2 vessel after the accident (Figure 17).

In this calculation, only 2 tons of magma components are slumping into the lower head (Figure 20) compared to 20 tons in real accident. This low value results from the too high level into the core (Figure 15) after the stop of the primary pumps and to the inactivation of debris model into the core area.

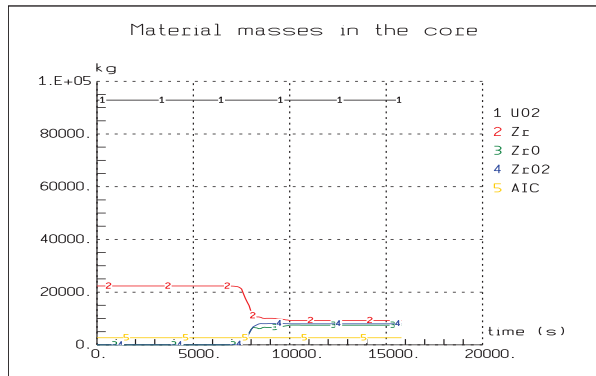


Figure 22 : Mass of components in the core

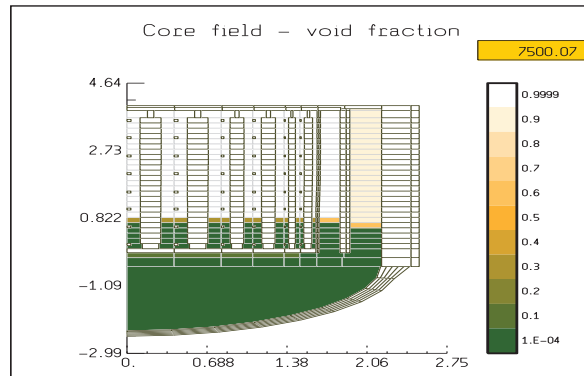


Figure 23: Void fraction in the core at 7500s

At time 8520s, the origin of the break was found by an operator. PORV was manually closed (Figure 11, evolutions 5,6) and core level increased again thanks to make up mass flow rate (Figure 11, evolution 1). At time 10440s GMPPB started again in order to reflood the core and to stop the degradation. Hydrogen production during the reflooding phase is stopped (Figure 19,22,23,24,25,26) because clads were ever oxidized above water level. Furthermore liquid water vaporization leads to an increase of primary pressure (Figure 12) up to PORV opening at time 11548s.

At time 12000s, safety injections are activated and temperature increase into the core is stopped immediately.

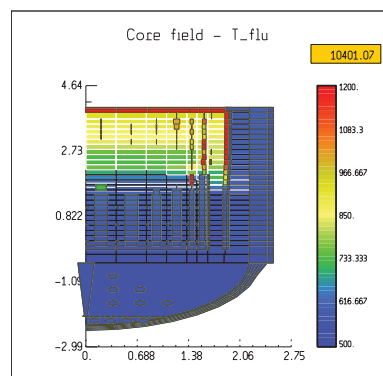


Figure 24 : Core temperature before reflooding

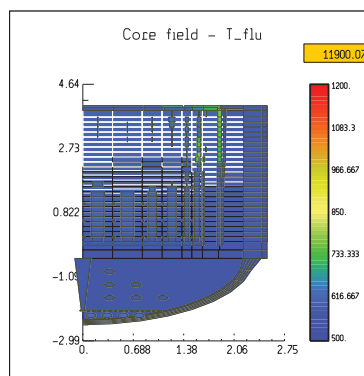


Figure 25 : Core temperature before reflooding

A PORV opening was necessary in order to decrease again the primary pressure ($t=11548$ s). At time 12000s, safety injections started again in order to reflood the core.

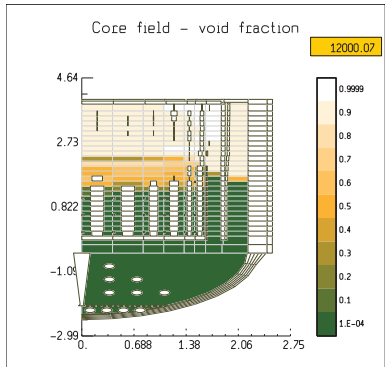


Figure 27 : void fraction in the vessel before SI reflooding

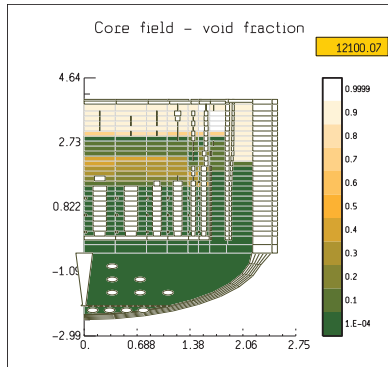


Figure 28 : void fraction in the vessel after SI reflooding

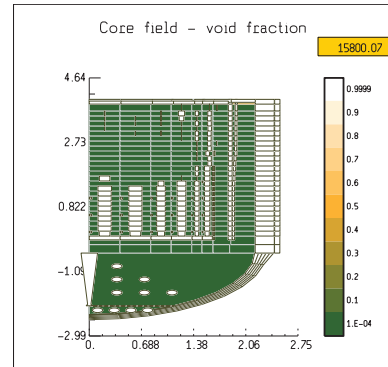


Figure 29 : void fraction in the vessel (end of calculation)

This validation reveals a general good agreement between ASTEC V2.1 calculation and TMI-2 real scenario measured values. The first significant difference comes from the pressurizer behavior just after the stop of GMPPs. Indeed an important mass of water coming from pressurizer is released in the hot leg. The second main difference comes from total mass of relocated materials into the lower head. Indeed Astec codes estimates 2 tons of corium into the lower head instead of 25 tons in the reality. These differences can be explained by inactivation of debris components in the ASTEC calculation, knowing that an important mass of debris should be created during the quenching of the core. This effect is important because debris slumping into the lower head should have an effect on the liquid water vaporization in the lower head, and as a consequence to the liquid core level, and hydrogen production. The total mass of molten materials calculated by ASTEC V2.1 is close to 60 tons (45-55 tons in real scenario). Hydrogen production is equal to 340 kg. Time calculation for this scenario is about 2 days.

5. CONCLUSION

This study aims at validating and assessing the ASTEC V2.1 new reflooding model. The first step was a validation on the PERICLES experimental facility named, and the general agreement on water level evolution and clad temperatures at several elevations was very good for both high and low pressure tests. The second step was the use of this model on a more complex application like a power plant calculation, here the real TMI-2 accident. This complex calculation revealed a thermal-hydraulic behavior of the code in very good accordance with data. Moreover, degraded configurations were simulated in agreement with observations done after the analysis of the TMI-2 vessel, like a cavity formation in the upper part of the core, a molten pool in the medium part, intact rods in the lower part, slumping of corium in the lower plenum through the bypass and total mass of corium formation.

In a numerical point of view, the time calculation for TMI-2 scenario revealed no numerical difficulties, and calculation was lower than 2 days CPU time.

An evolution to come of the reflooding model is a switch to another model currently in development and exclusively devoted to both porous media and debris bed, and in general well adapted to severely degraded situations.

The quench front progression appears to be well predicted. The time evolution of the cladding temperature during reflooding is also well reproduced. The model appears suitable for calculations of reflooding under various conditions (pressure, inlet velocity) and may be adapted to any code using large meshes, as it is the case for codes used to simulate severe accidents.

REFERENCES

- [1] Chatelard P., Reinke N., Arndt S., Belon S., Cantrel L., Carenini L., Chevalier-Jabet K., Cousin F., Eckel J., Jacq F., Marchetto C., Mun C., Piar L., “ASTEC V2 severe accident integral code main features, current V2.0 modeling status, perspectives”, Nuclear Engineering and Design, 272 (June 2014), p.119-135
- [2] P.DRAI & all, “ICARE/CATHARE V2.3rev1-User’s manual and guidelines”, IRSN technical report DPAM-SEMCA-2010-398 (January 2011)
- [3] Chikkhi N., Fichot F., “Reflooding model for quasi-intact rod configuration: Quench front tracking and heat transfer closure laws”, Nuclear Engineering and Design, Vol.240 (2010), p-3387-3396
- [4] Veteau J.M, Digonnet A , “PERICLES Program: Boil-up, Boil-off and Reflooding High Pressure Experiments in a PWR assembly”, Technical report, CEA FRANCE ref Seth/LES/89-74, 1989
- [5] Ergun, S., “Advanced modeling of dispersed flow film boiling with two flow, five field Eulerian – Eulerian Approach and Effects of Spacer Grids on Heat Transfer”, PhD, The Pennsylvania State University, Mau 2006
- [6] P.Ruyer&all, “CFD Study of Mist Flow Wall Heat Transfer Downstream The Quench Front During Reflood Stage of LOCA” Conference NURETH 15, paper number 23, Pisa,Italy,May 2013
- [7] Lavialle G. “CATHARE 2 V25.1, Physical laws used in the reflooding sub-module”, CEA, 2005
- [8] Ishii, M., De Jarlais, G., 1986. “ Flow regime transition and interfacial characteristics of inverted annular flow”. Nuclear Engineering and Design 95, 171–184.
- [9] Draï , P. “Validation du code ASTEC V2.1 sur les essais PERICLES – Partie deux : tests de renouage de cœur, IRSN, 2014
- [10] Laborde, L. “Validation of ASTEC V2.1 based on QUENCH-03 and QUENCH-11 experiments”, Technical Report IRSN,, 2014-412
- [11] Broughton, J., Kuan, P., Petti, D., Tolman, E., 1989. A scenario of the Three Mile Island unit 2 accident. Nuclear Technology 87, 34–53.